2014

High Precision Three-body Variational Method for Critical Nuclear Charge

Michael A. Busuttil
University of Windsor

High Precision Three-body Variational Method for Critical Nuclear Charge

by

Michael A Busuttil

A Thesis
Submitted to the Faculty of Graduate Studies
through the Department of Physics in Partial Fulfillment
of the Requirements for the Degree of Master of Science at the
University of Windsor

Windsor, Ontario, Canada
2014

High Precision Three-body Variational Method for Critical Nuclear Charge

by

Michael A Busuttil

APPROVED BY:

S. Rehse
Department of Physics

G. W. F. Drake, Advisor
Department of Physics

R. Frost
School of Computer Science

17 Jan 2014

Author's Declaration of Originality

I hereby certify that I am the sole author of this thesis and that no part of this thesis has been published or submitted for publication.

I certify that, to the best of my knowledge, my thesis does not infringe upon anyones copyright nor violate any proprietary rights and that any ideas, techniques, quotations, or any other material from the work of other people included in my thesis, published or otherwise, are fully acknowledged in accordance with the standard referencing practices. Furthermore, to the extent that I have included copyrighted material that surpasses the bounds of fair dealing within the meaning of the Canada Copyright Act, I certify that I have obtained a written permission from the copyright owner(s) to include such material(s) in my thesis and have included copies of such copyright clearances to my appendix.

I declare that this is a true copy of my thesis, including any final revisions, as approved by my thesis committee and the Graduate Studies office, and that this thesis has not been submitted for a higher degree to any other University or Institution.

Abstract

For an atom there exists a critical nuclear charge Z_c that is just sufficient to bind the nucleus and its electrons into a stable configuration. A study of the critical charge for two-electron atoms is presented with the purpose of improving accuracy for Z_c. To this end, high precision techniques involving the variational method with multiple basis sets in Hylleraas coordinates are employed. The method is particularly well adapted to the case where one electron is strongly bound and the other is at the limit of becoming unbound. The results are analysed in terms of fractional powers of $(Z - Z_c)$ related to the analytic structure of the energy $E(Z)$ and a $1/Z$ expansion for the energy. This results in a Z_c of 0.911 028 08(5). Future work prompted by this study includes development of direct techniques to determine Z_c utilizing the method's low-Z stability; developing the framework and mathematical justification for a novel bootstrap analysis method used in curve-fitting; and investigating the inclusion of finite nuclear mass, relativistic effects, and other higher order corrections in the determination of Z_c.

To my father, Tony Busuttil, for instilling in me the love for education, for showing me the need for unconventional thinking, and for leading me toward the joy that is scientific research.

Acknowledgements

This work would not have been possible without support from my adviser and mentor, Dr. Gordon Drake. Dr. Drake has always pushed me to strive for better both in the lab and in life and I am truly grateful for the broad range of skills he's helped me to develop. It has been an honour to learn and grow under the supervision of such an established and respected member of the scientific community. Gordon has been instrumental in the advancement of my career and I count myself as extremely lucky to have had the experience of working as one of his students. I also wish to thank him, the University of Windsor Department of Physics, and Daresbury National Laboratory (Cheshire, UK) for providing me with financial support through teaching and research assistantships throughout my studies. The people I've met and worked with through these institutions like Dr. Gordon Drake, Dr. Dominic Seccombe, Dr. Tim Reddish, Dr. Nigel Poolton, and Dr. David Quin are all world class scientists and have helped to shape me into the person I strive to be.

I would also like to acknowledge my friends and colleagues, especially Amirreza Moini, Eva Schulhoff, Dmitry Gavrilov, Behnam Javanparast, Lauren Moffatt, Camille Estienne, Qixue (Charles) Wu, Dominic Seccombe, and the rest of my classmates and group members for the unforgettable experiences and willingness to exchange skills and knowledge with me - especially in times when that exchange tilted heavily in my favour.

Finally, I would like to thank my family, the close-knit group of families I grew up with, and the good people at All Saints' Church. It is so much easier and much more fulfilling

to succeed when you have so many people rooting for your success and drinking to your accomplishments.

To all the positive people in my life, I am eternally grateful for all the support.

Contents

List of Figures

List of Tables

Chapter 1

Introduction

For an atom there exists a critical nuclear charge Z_c that is just sufficient to bind the nucleus and its electrons into a stable configuration. This work seeks to resolve the disagreement in the value of Z_c for the two-electron case as investigated by Baker [1] and Guevara [2] and establish an associated interval of confidence.

The helium atom is a thoroughly studied example of the three-body problem, consisting of a nucleus and two planet-like electrons. The interaction between constituent particles can be modelled to a first approximation by considering the nucleus to be infinitely massive and neglecting the interaction of the electrons with one another. With the electrons immersed in the Coulomb field of the nucleus alone, and neglecting the Coulomb repulsion between electrons, the energy of the system can be solved exactly with the use of the Schrödinger Equation. The solution for this crude model yields energies that deviate by over 25% ($\sim$ 30eV) from experimental observations which lie far beyond the range of accuracy needed for this study.

The inclusion of the electron-electron interaction into the model greatly improves agreement at the expense of increased computer time and mathematical analysis. An exact analytic solution to yield the energy does not exist for this model but an essentially exact numerical solution can be found which is accurate enough for all practical purposes. Such

a solution is obtained through creative use of the Variational Method with specially constructed basis sets of functions. The basis sets proposed by Hylleraas [3] can be extended to accurately describe both the long-range and short-range behaviour of the electrons. These functions combined with methods developed by Drake et al. [4] give nonrelativistic energies with accuracies better than 1 part in 10^{20}.

Future work could see the atomic model extended to include relativistic effects, finite nuclear mass, and other higher order corrections. Exhaustive inclusion yields experimental agreement in the peV range which even allows for nuclear fine structure comparisons from these in-depth atomic calculations [5]. While this degree of accuracy is beyond the scope of the present work, the study establishes a method which can be easily extended to include an atomic model which considers these higher order perturbations.

With the model yielding sufficiently accurate energies (E) as a function of nuclear charge (Z) the critical nuclear charge (or critical charge, Z_c) can be investigated. The critical charge is the nuclear charge at which one of the electrons is at the limit of becoming unbound to the nucleus and the three-body atom ceases to be a stable configuration. The critical charge can then be found through curve-fitting to a series expansion for E as a function of Z about the point Z_c. This motivates the evaluation of energy as close as possible to Z_c to minimize the uncertainty. Application of the variational method is not straightforward in this critical charge limit where Guevara observes convergence issues [2]. The use of Hylleraas functions are employed for this study and serve to alleviate convergence problems thus allowing for energy evaluation much closer to Z_c. Curve-fitting is performed using these high-accuracy data points alongside the bootstrap method of sampling residuals to obtain the interval of confidence for Z_c.

Z_c for the two-electron case case can be applied to all electronic configurations through use of the ubiquitous $1/Z$ expansion. The value of Z_c serves not only as the critical charge for two-electron atoms but also as the radius of convergence for the $1/Z$ expansion [1]. This dictates the convergence of the series and lends to the investigation on the functional dependence of atomic energy with charge $E(Z)$. This function $E(Z)$ can be studied in the complex plane where its analytic structure can be explored. Investigations surrounding Z_c

also shed light onto the methods through which the wave functions are generated. Expected wave function behaviour as the outer electron becomes unbound provides a meaningful way to compare different methods of wave function generation in this critical charge limit.

Chapter 2

Theory

2.1 The Atomic Model and its solution

Modelling the helium atom as three nonrelativistic charged particles yields energies of sufficient accuracy. Energies are obtained through solving the Schrödinger equation $[H\Psi = (T+V)\Psi = E\Psi]$ for the three-particle system:

$$\left(-\frac{\hbar^2}{2M}\nabla^2_{\mathbf{R}_0} - \frac{\hbar^2}{2m}\nabla^2_{\mathbf{R}_1} - \frac{\hbar^2}{2m}\nabla^2_{\mathbf{R}_2} - \frac{Ze^2}{4\pi\epsilon_0|\mathbf{R}_0-\mathbf{R}_1|} - \frac{Ze^2}{4\pi\epsilon_0|\mathbf{R}_0-\mathbf{R}_2|} + \frac{e^2}{4\pi\epsilon_0|\mathbf{R}_1-\mathbf{R}_2|}\right)\Psi = E\Psi \tag{2.1}$$

for nucleus of charge Ze, mass M, and position $\mathbf{R}_0$ and electrons of charge e, mass m, and positions $\mathbf{R}_1$ and $\mathbf{R}_2$. The remainder of this section will focus on solving this equation.

2.1.1 Change of Coordinates: restating the problem

Our first step in solving Eq. (2.1) is to describe the contained distances relative to the system's centre of mass as was done in Bohr's treatment of the hydrogen problem. Solutions are found in the centre of mass frame where the displacement of the centre of mass from

the origin is written as

$$\mathbf{R} = \frac{M\mathbf{R}_0 + m\mathbf{R}_1 + m\mathbf{R}_2}{(M+2m)},$$

the distance between particles (Fig. 2.1) is written as

$$\begin{aligned}\mathbf{r}_1 &= \mathbf{R}_1 - \mathbf{R}_0,\\ \mathbf{r}_2 &= \mathbf{R}_2 - \mathbf{R}_0,\\ \mathbf{r}_{12} &= \mathbf{R}_2 - \mathbf{R}_1,\end{aligned}$$

and the differential operators are replaced with the square of the following operators [6]:

$$\begin{aligned}\vec{\nabla}_{\mathbf{R}_0} &= \frac{M}{M+2m_e}\vec{\nabla}_{\mathbf{R}_{CM}} - \vec{\nabla}_{\mathbf{r}_1} - \vec{\nabla}_{\mathbf{r}_2},\\ \vec{\nabla}_{\mathbf{R}_1} &= \frac{m_e}{M+2m}\vec{\nabla}_{\mathbf{R}_{CM}} - \vec{\nabla}_{\mathbf{r}_1},\\ \vec{\nabla}_{\mathbf{R}_2} &= \frac{m_e}{M+2m_e}\vec{\nabla}_{\mathbf{R}_{CM}} - \vec{\nabla}_{\mathbf{r}_2}.\end{aligned}$$

This results in the transformation of Eq. (2.1) to the centre of mass Schrödinger Equation:

$$\begin{aligned}\left(-\frac{\hbar^2}{2}\left[\left(\frac{1}{M+2m}\right)\nabla^2_{\mathbf{R}} + \left(\frac{1}{M}+\frac{1}{m}\right)\nabla^2_{\mathbf{r}_1} + \left(\frac{1}{M}+\frac{1}{m}\right)\nabla^2_{\mathbf{r}_2}\right.\right.\\ \left.\left. -\frac{2}{M}\vec{\nabla}_{\mathbf{r}_1}\cdot\vec{\nabla}_{\mathbf{r}_1}\right] - \frac{Ze^2}{4\pi\epsilon_0 r_1} - \frac{Ze^2}{4\pi\epsilon_0 r_2} + \frac{e^2}{4\pi\epsilon_0 r_{12}}\right)\Psi = E\Psi. \qquad (2.2)\end{aligned}$$

Simplification is performed by recognizing that $\nabla^2_{\mathbf{R}}$ is related to the system's acceleration which of course vanishes in the absence of external forces. For further simplification the reduced mass $\mu = mM/(m+M)$ and Bohr radius $a_\mu = (m/\mu)a_0 = 4\pi\epsilon_0\hbar^2/\mu e^2$ are introduced so that the distances may be scaled accordingly:

$$\begin{aligned}r_i &\rightarrow r_i a_\mu\\ \nabla_{\mathbf{r}_i} &\rightarrow \nabla_{\mathbf{r}_i}/a_\mu. \qquad (2.3)\end{aligned}$$

These steps reduce Eq. (2.2) and give

$$\frac{e^2}{4\pi\epsilon_0 a_\mu}\left[-\frac{1}{2}\nabla_1^2 - \frac{1}{2}\nabla_2^2 + \frac{\mu}{M}\vec{\nabla}_{\mathbf{r}_1}\cdot\vec{\nabla}_{\mathbf{r}_1} - \frac{Z}{r_1} - \frac{Z}{r_2} + \frac{1}{r_{12}}\right]\Psi = E\Psi \qquad (2.4)$$

where $\nabla_i = \nabla_{\mathbf{r}_i}$.

It is here that a somewhat significant approximation is made; namely that the nuclear mass is assumed infinitely heavy. This dismisses the mass-polarization $\vec{\nabla}_{\mathbf{r}_1} \cdot \vec{\nabla}_{\mathbf{r}_1}$ term as $\mu/M \to 0$. This assumption results in the infinite nuclear mass three-body Schrödinger equation:

$$\boxed{\left\{-\frac{1}{2}\nabla_1^2 - \frac{1}{2}\nabla_2^2 - \frac{Z}{r_1} - \frac{Z}{r_2} + \frac{1}{r_{12}}\right\}\Psi = E\Psi} \tag{2.5}$$

where the energy E is measured in units of $e^2/4\pi\epsilon_0 a_\mu$ (atomic units).

2.1.2 The Variational Principal: method of solution

Solutions to Eq. (2.5) are obtained through application of Schrödinger's Variational Principal. This remarkably useful quantum mechanical tool is accurately described by Griffiths [7] as "extraordinarily powerful and embarrassingly easy to use". With a given Hamiltonian and any arbitrary normalizable wave function, the method will yield an energy that is proven [8] to be an upper bound to the actual energy of the given system described in the Hamiltonian:

$$E_{trial} = \frac{\langle\psi|\mathbf{H}|\psi\rangle}{\langle\psi|\psi\rangle} \geq E_{actual} \tag{2.6}$$

This allows for the determination of optimum values for Energy, E_{trial}, given the parametrized (or trial) wave function, ψ, by simply finding the lowest energy result. Trial wave functions which bear closer resemblance to the true wave function will achieve a lower energy while requiring less parameters and fewer numbers of terms (Sect. 2.1.3).

Since E_{trial} (or simply E) will always be greater than or equal to the actual energy, the minimization of E is the objective in the search for the optimal energy solution. To this end the trial function ψ (Eq. 2.8) is constructed with a set of parameters a_i with respect to which E will be minimized, resulting in a system of homogeneous equations:

$$\frac{\partial E}{\partial a_i} = 0. \tag{2.7}$$

2.1.3 Functional form of ψ the solution

The trial function used in the evaluation of Eq. (2.6) is one adapted from Hylleraas [3] with a doubled basis set as proposed by Drake [9] of functional form

$$\psi = \sum_{n=1}^{2} \sum_{ijk} a_{ijkn} r_1^i r_2^j r_{12}^k e^{-\alpha_n r_1 - \beta_n r_2} \tag{2.8}$$

with linear coefficients a_{ijkn}, nonlinear parameters α_1, β_1, α_2, β_2, and particle separations r_1, r_2, and r_{12}. The set of basis functions is doubled by introducing a second pair of nonlinear parameters (α_2, β_2) where each pair of parameters can be optimized to represent different distance scales.

The total number of terms is given by the summation limits on integers i, j, and k which if allowed to sum to infinity is proven to ensure the spanning of Hilbert space for ψ [10, 11]. Of course in practice the infinite horizon is unattainable so decisions need to be made regarding which terms to include and which to omit. Three primary factors must be considered when selecting terms; computation time, linear dependency, and effect on energy. Computation time is minimized by minimizing the term count in the trial wave function (N) since the time bottleneck in energy calculation is the diagonalization of $N \times N$ matrices. Linear dependency issues arise when numerical evaluation of matrix elements for different terms yield the same result to the precision of the memory registers. Computational strategies can be employed to deal with these effects including the increase in register size but the selection of appropriate terms resulting in the greatest change in final energy is the best first step. A systematic guideline for choosing terms is the imposition of a maximum exponent Ω (often called the Pekeris shell) and enforcement of exponent uniqueness to establish the bounds

$$\begin{aligned} i + j + k &\leq \Omega \\ i &< j, \end{aligned} \tag{2.9}$$

giving a total number of terms $N \approx (\Omega+1)(\Omega+2)(\Omega+3)/3$. This strategy has been shown in practice to be an optimal choice for functions with a single pair of nonlinear parameters

[4] but is not proven so. The best methods for choosing terms are found through simple trial and error and sometimes aided by intuition. Such intuition proved fruitful with the extension of term counts by increasing the number of nonlinear parameters. It should be noted that lessons learned in picking terms for single basis sets do not always extend to multiple basis sets and caution must be exercised in these regimes where linear dependencies can creep into results.

Doubling of the basis functions through doubling of the nonlinear parameters allows for better description of the actual wave function behaviour especially as electrons occupy different regions of space. The nonlinear parameters dictate the radial decay in electron probability and as such can be optimized to cover both long range and short range behaviour when doubled. This allows for fewer terms to give the same energy precision thus lowering computation time while avoiding numerical linear dependence.

2.1.4 Integrals and Operators solution evaluation

The evaluation of Eq. (2.6) involves computation of volume integrals for the Hamiltonian of Eq. (2.5) acting on the trial function ψ of Eq. (2.8). This requires an expression for the Laplacian and construction of integrals in the Hylleraas coordinate system (Fig. 2.1). The Laplacian [12, 13] gives rise to the final Hamiltonian

$$\begin{aligned} H = &- \frac{\frac{\partial}{\partial r_1}\left(r_1^2\left(\frac{\partial}{\partial r_1}\right)\right)}{2r_1^2} - \frac{\frac{\partial}{\partial r_2}\left(r_2^2\left(\frac{\partial}{\partial r_2}\right)\right)}{2r_2^2} - \frac{\frac{\partial}{\partial r_{12}}\left(r_{12}^2\left(\frac{\partial}{\partial r_{12}}\right)\right)}{r_{12}^2} \\ &- \frac{\left(r_1 - \frac{r_1^2 + r_2^2 - r_{12}^2}{2r_1}\right)\left(\frac{\partial}{\partial r_{12}}\left(\frac{\partial}{\partial r_1}\right)\right)}{r_{12}} - \frac{\left(r_2 - \frac{r_1^2 + r_2^2 - r_{12}^2}{2r_2}\right)\left(\frac{\partial}{\partial r_{12}}\left(\frac{\partial}{\partial r_2}\right)\right)}{r_{12}} \\ &- \left(\frac{1}{r_1} + \frac{1}{r_2} - \frac{1}{Zr_{12}}\right) \end{aligned} \tag{2.10}$$

while simplification of the volume element and integration limits gives rise to the sum of

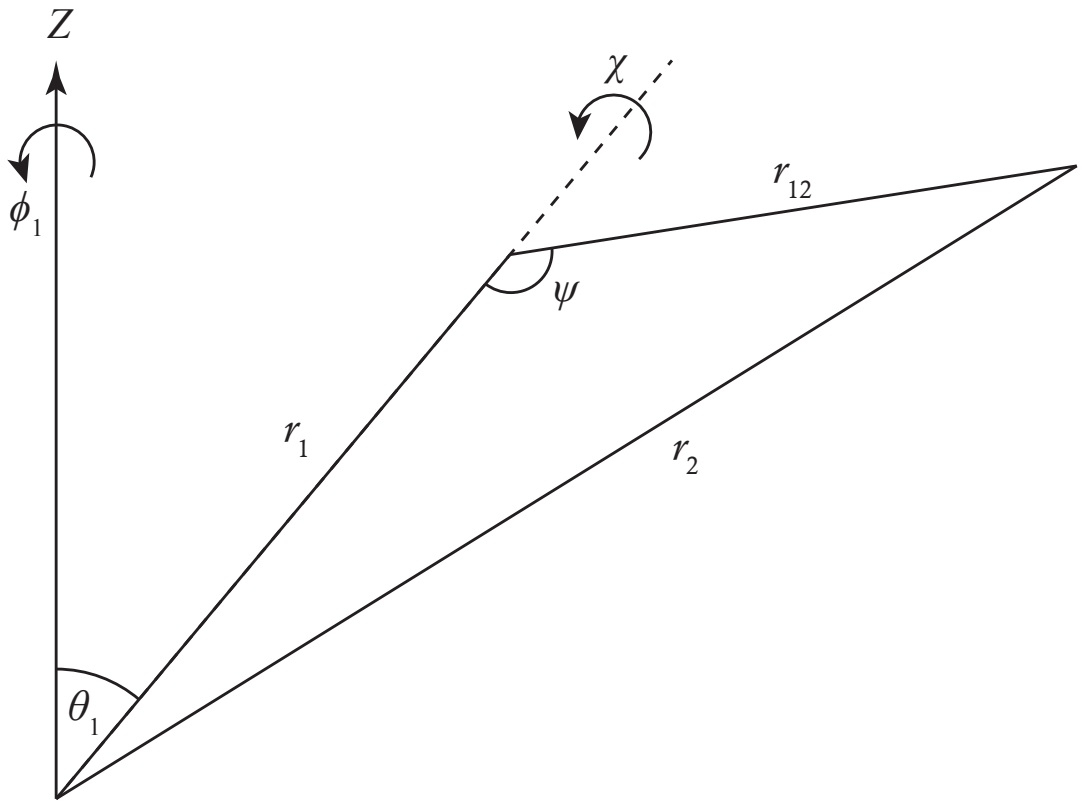

Figure 2.1: Hylleraas coordinate system.

two triple integrals requiring evaluation [14]:

$$\left\{\int_0^\infty e^{-\gamma r_1} r_1 dr_1 \int_{r_1}^\infty e^{-\gamma r_2} r_2 dr_2 \int_{r_2-r_1}^{r_2+r_1} r_{12} dr_{12} + \int_0^\infty e^{-\gamma r_2} r_2 dr_2 \int_{r_2}^\infty e^{-\gamma r_1} r_1 dr_1 \int_{r_1-r_2}^{r_1+r_2} r_{12} dr_{12}\right\}. \tag{2.11}$$

These integrals are straightforward and easily implemented by machines through use of

$$\int_{r_b}^\infty e^{-\gamma r_a} r_a^n dr = \gamma^{-n+1} n! e^{-\gamma r_b} \sum_{k=0}^{n} \frac{(\gamma r_b)^k}{k!} \tag{2.12}$$

which can be calculated as needed or pre-calculated and stored in tables [9] for even faster run-time performance.

2.2 Energy Extrapolation

The goal of this section is to estimate a value which is described exactly by an infinite number of terms but where only a finite number of terms are feasibly attainable. The case used in this study is the calculation of atomic energy whose computation time is proportional to N^3 (where N is the number of terms). It is this N^3 time-dependence that imposes the limitation on term count. Analysis of the first 20 term counts for the atomic energy of H^- ($Z = 1.0$) shows the energy differences in successive term counts, $E_\Omega - E_{\Omega-1}$, becoming increasingly smaller (Table 2.1). The rate at which these differences shrink (the

Table 2.1: Convergence of the atomic energy for the ground state of two-electron Hydrogen

Ω	N	E_Ω	$E_\Omega - E_{\Omega-1}$	R
8	189	−0.527 751 016 314 715 469		
9	248	−0.527 751 016 497 134 491	−0.000 000 000 182 419 022	
10	317	−0.527 751 016 534 132 818	−0.000 000 000 036 998 326	4.930
11	398	−0.527 751 016 541 953 536	−0.000 000 000 007 820 717	4.730
12	490	−0.527 751 016 543 812 716	−0.000 000 000 001 859 180	4.206
13	596	−0.527 751 016 544 209 984	−0.000 000 000 000 397 267	4.679
14	714	−0.527 751 016 544 333 933	−0.000 000 000 000 123 949	3.205
15	848	−0.527 751 016 544 362 023	−0.000 000 000 000 028 090	4.412
16	995	−0.527 751 016 544 372 770	−0.000 000 000 000 010 746	2.613
17	1 160	−0.527 751 016 544 375 399	−0.000 000 000 000 002 628	4.087
18	1 339	−0.527 751 016 544 376 603	−0.000 000 000 000 001 204	2.183
19	1 538	−0.527 751 016 544 376 933	−0.000 000 000 000 000 330	3.648
20	1 752	−0.527 751 016 544 377 097	−0.000 000 000 000 000 164	2.009
∞		−0.527 751 016 544 377 32(6)		

ratio of differences, R) is approximately constant and this constant shrinking is assumed to continue to infinity. The series can be summed to infinity if R is constant and greater than

1 using the geometric series. This is expressed with energy difference, $D = E_n - E_{n-1}$, and difference ratio reciprocal, $r = \frac{1}{R} = \frac{E_{n-1}-E_{n-2}}{E_n-E_{n-1}}$, to give an extrapolated energy

$$\begin{aligned} E_\infty &= E_{20} + \sum_{n=1}^{\infty} D r^{n-1} \\ &= E_{20} + \frac{D}{1-r}. \end{aligned} \tag{2.13}$$

The average shrink ratio, $\langle r \rangle$, is used to extrapolate from the highest attained term count out to the infinite term count and the standard deviation in the ratio (σ_r) gives the extrapolated uncertainty:

$$\delta E_\infty = \left| \frac{D}{1-(\langle r \rangle + \sigma_r)} - \frac{D}{1-(\langle r \rangle - \sigma_r)} \right|. \tag{2.14}$$

2.3 Computationally simplified nonlinear fit

This study requires fitting data to Puiseux expansion functions ($\sum_n a_n T^{n/k}, k \in \mathbb{Z}$) of different fractional powers and variable numbers of terms (N):

$$\begin{aligned} E(Z; Z_c, a_1, .., a_N) &= -Z_c^2/2 + a_1(Z-Z_c)^{1/2} + a_2(Z-Z_c)^{2/2} + \cdots + a_N(Z-Z_c)^{N/2} \\ &= -Z_c^2/2 + \sum_{n=1}^{N} a_n (Z-Z_c)^{n/2}, \end{aligned} \tag{2.15}$$

with $N+1$ terms, 1/2-integer powers, and parameters $a_1 \ldots a_N$ and Z_c.[1] This function can be transformed to a simple N-degree polynomial by applying two straightforward transformations to both the data and the function:

$$\begin{aligned} E_T(Z) &= E(Z) + \frac{Z_c^2}{2}, \\ X &= (Z-Z_c)^{1/2}. \end{aligned} \tag{2.16}$$

[1] The current study analyzes full-integer, 1/2-integer, and 1/3-integer power fittings for terms counts from $N = 2$ to 20.

This gives the transformed energy,

$$\begin{aligned} E_T(Z) &= E(Z; Z_c, a_1, .., a_N) + \frac{Z_c^2}{2} \\ &= a_1(Z - Z_c)^{1/2} + a_2(Z - Z_c)^{2/2} + \cdots + a_N(Z - Z_c)^{N/2} \\ &= a_1 X^1 + a_2 X^2 + \cdots + a_N X^N \\ E_T(X; a_1, .., a_N) &= \sum_{n=1}^{N} a_n X^n, \end{aligned} \tag{2.17}$$

which is a simple polynomial of degree N with the constant term a_0 omitted. The transformed data is then fit by the method of least squares to an N-degree polynomial of form

$$E_{fit}(X; c_0, .., c_N) = \sum_{n=0}^{N} c_n X^n, \tag{2.18}$$

where the constant term a_0 is present. This fit will yield an optimized value of zero for parameter a_0 with the correct choice of Z_c. Exploiting this property allows iterative deduction of Z_c through a successive trial and fitting procedure.

For this procedure Newton's method is employed to find the x-intercept for a_0 as a function of Z_c. An initial guess of Z_c, $Z_{c,0}$, is made for which the data is transformed according to Eq. (2.16) and fit by the method of least squares to an N-degree polynomial in order to yield a_0. The slope of $a_0(Z_c)$ at $Z_{c,0}$ is determined by repeating this fit at both $Z_{c,0} - \delta Z$ and $Z_{c,0} + \delta Z$ for a $\delta Z = .0001$ thus obtaining 2 more a_0 values from which the slope is simply $m_0 = {}^{\Delta a_0}/_{2\Delta Z}$. The new x-intercept is then calculated from Newton's method to be $Z_{c,1} = Z_{c,0} - a_0(Z_{c,0})/m_0$. This entire process is then repeated until the difference between successive $Z_{c,n}$'s is sufficiently small, namely one thousandth of the greatest uncertainty inherent in the data (approximately 10^{-18}).

2.4 Bootstrap standard error for curve fitting

The bootstrap is a method of resampling a finite data set to obtain statistics such as the sample mean and associated interval of confidence. It is a straightforward brute force method of great utility especially when analytic statistical inference requires a complex derivation and all sources of uncertainty may not be known. This alternative method

is used to generate sample statistics where computational power is replaced with careful analytics to yield the same result giving a method which is mathematically justified [15] with considerably less effort required for implementation.

The analysis of this study requires that an interval of confidence be established for a parameter used in the fitting procedure of section 2.3, namely parameter Z_c. The bootstrap process for this boils down to an initial calculation followed by a repeated perturbation then recalculation. First, the best fit is initially calculated using the given extrapolated energies which results in residual differences between the fitted $E(Z)$ and each energy data point (the initial calculation). These residuals are randomly added or subtracted (with replacement) to each energy point along with a random deviation within the point's uncertainty (the perturbation). The best fit is again calculated now with the perturbated data points where the resulting Z_c is included in a histogram of samples. This perturbation then calculation procedure is repeated for roughly 300 iterations to gain reliable statistics resulting in the critical nuclear charge and its associated interval of confidence.

Chapter 3

Method

Determination of the critical nuclear charge is a multistage process that can be broken down into three fundamental steps: calculating energy, extrapolating results, and bootstrapping the statistics. First a set of nuclear charges is slated for investigation and then the following procedure is implemented:

3.1 Energy Calculation

Once a given charge is selected for energy calculation the variational method of section 2.1.2 is applied. The charge Z dictates the Hamiltonian (Eq. 2.5) and Ω dictates the number of terms in the wave function (Eq. 2.8). These calculations can take anywhere from milliseconds in the case of ~ 200 terms ($\Omega = 8$) to several minutes in the case of $\sim 1,800$ terms ($\Omega = 20$). Increasing Ω means increasing accuracy at the expense of computational time so for infinite accuracy one would require infinite time. To overcome this hurdle the infinite accuracy solution is estimated by extrapolation using the method described in section 2.2. This requires converged energies for a set of Ω (wave function term counts, $\Omega = 8 \ldots 20$ in our case) to yield energies with associated uncertainties which are then used to determine the best fit for the parametrized $E(Z, Z_c)$ function.

3.2 Curve Fitting

The $E(Z, Z_c)$ functions used for fitting are Puiseux expansions of different fractional powers and variable numbers of terms (N):

$$\begin{aligned} E(Z; Z_c, a_1, .., a_N) &= -Z_c^2/_2 + a_1(Z - Z_c)^{1/_2} + a_2(Z - Z_c)^{2/_2} + \cdots + a_N(Z - Z_c)^{N/_2} \\ &= -Z_c^2/_2 + \sum_{n=1}^{N} a_n(Z - Z_c)^{n/_2}, \end{aligned} \tag{3.1}$$

with $N + 1$ terms, $^1/_2$-integer powers, and parameters $a_1 \ldots a_N$ and Z_c.[1] This nonlinear fit is arduous, time consuming (tens of minutes per fit), and includes terms with imaginary numbers for $Z < Z_c$ but with some algebraic manipulation it can be modified into a form which alleviates these computational headaches. The substitution of $E_T(Z) = E(Z) + Z_c^2/_2$ and $X = (Z - Z_c)^{1/_2}$ as described in section 2.3 yields a function that takes seconds to fit thus allowing for a more practical implementation of bootstrap uncertainty analysis.

3.3 Bootstrap

The statistical method known as the bootstrap provides a straightforward procedure for determining intervals of confidence for each Z_c resulting from the varying Puiseux fits. The process involves the curve fitting procedure of section 2.3 repeated for 300 perturbations of the input data set described in section 2.4. It greatly simplifies the error analysis by replacing a thorough mathematical treatment with brute force computation requiring only minutes to perform.

[1] The current study analysis full-integer, $^1/_2$-integer, and $^1/_3$-integer power fittings for terms counts from $N = 2$ to 20.

Chapter 4

Computational Machinery

The method outlined in this study is implemented in practice with the use of computers. Data is transferred between computational stages and visualized for analysis through the programming of functions, modules, and scripts which are briefly described here. The three primary stages of the implementation are atomic energy harvesting, atomic energy refinement, and fitted curve extrapolation with quality control and analysis being performed before, during, and after each phase. The programs are divided by file and briefly described below and in Table 4.1 with the enveloping architecture outlined in Fig. 4.1.

The first stage controls the harvesting of atomic energies for selected nuclear charges. The calculation of atomic energies and wave function parameters is done in the FORTRAN program Dpoldlz.f which takes as input the wave function term count (Ω), the nuclear charge (Z), and optional initial guesses for nonlinear parameter values and their derivatives. This is the machine implementation of Sect. 2.1. The program uses an iterative method to optimize the nonlinear parameters and as a result will require less time to complete if given good initial guesses. The code is borrowed from the machine implementation of the Helium problem done in Dr. Gordon Drake's research group which has evolved over the years from its original punch-card version and has been modified in this work to allow for non-integer Z. A large volume of data is generated in this process where collection is

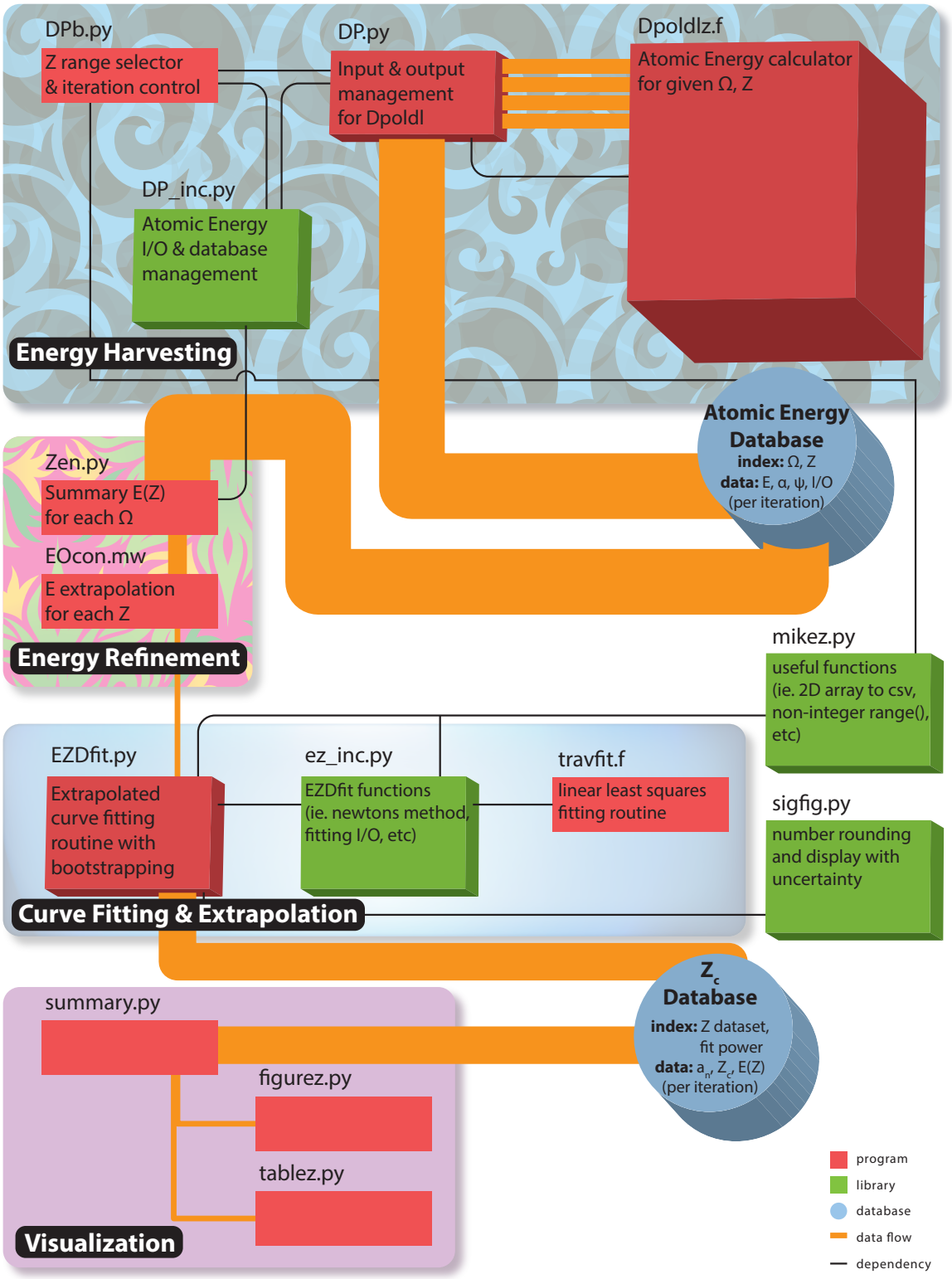

Figure 4.1: Visualization of computational programs and flow of data.

valued for use in the final analysis as well as in quality assurance to ensure stability of each individual resulting energy and parameter. Retention of this data is done through the wrapper Python script DP.py which takes as input the wave function term count (Ω) and nuclear charge (Z), subsequently executes Dpoldlz.f with these values, and then stores the result of each iteration in a database. This allows for post-execution scrutiny over results as well as the use of these results as the initial guesses for future calculation of atomic energy for slightly different nuclear charge or term count. This script relies on a library of functions to manage the database which can be found in dp_inc.py and is executed in mass for a batch of nuclear charges and term counts through the Python script DPb.py which also relies on the dp_inc.py library. This batch script takes as input a range of nuclear charges (Z) and range of term counts (Ω) for which the wrapper script DP.py is executed. The database is searched for initial guesses which would best suit the desired calculation and these results are served up as inputs for Dpoldlz.f. The major result from this section of the computation is the array of atomic energies for different nuclear charges and different wave function term counts. These will be used to estimate the uncertainty of the energy for each nuclear charge.

The second stage computes the extrapolated atomic energy for each nuclear charge from the collection of energies for each Ω. A table where each row corresponds to a nuclear charge and each column corresponds to a value of Ω is constructed with the Python script Zen.py from data in the atomic energy database. This table is piped to the Maple worksheet EOcon.mw where a convergence table as described in Sect. 2.2 is constructed and visualized for each nuclear charge. These convergence tables give the uncertainty bounds on each nuclear charge which is then tabulated (Table A.1) and exported as a comma separated value spreadsheet (file extension .csv) for input into the fitting and extrapolation routine.

The third and final stage performs the nonlinear fitting and extrapolation described in Sect. 3.2 as well as the bootstrap uncertainty analysis described in Sect. 3.3. This is all done in the python script EZDfit.py which relies on functions in the library ez_inc.py, the linear least squares fitting module travfit.f, and other libraries written exclusively for this project with plans for world-wide open source sharing and distribution. The program is

provided with input for the different subsets of nuclear charge data, the exponents for the Puiseux fit function, a range for the number of terms in the Puiseux series, and the Atomic energies with their uncertainties from the EOcon.mw worksheet. Each data set is fit with the different Puiseux functions 300 times each with slightly perturbated input energy data points in accordance with the bootstrap curve fitting method (Sect. 2.4) and found to require 4 iterations of a 3 point Newton's method variant to sufficiently converge. This yields a set of 300 fit parameters for each of the different Puiseux function term lengths (from 2 to 20) and fit powers ($1/3, 1/2$, and 1) for each of the 18 isolated data subsets to be saved for analysis. These resulting three million values ($300 \times (2 + 3 + 4 + \cdots + 20) \times 3 \times 18 \approx 3.4 \times 10^6$) are generated from roughly four million calls to the linear least squares fitting module ($300 \times 3 \times (20 - 1) \times 18 \times 4 \times 3 = 3\,693\,600$) and stored in a database where the primary quantity of interest is Z_c. The critical charge, Z_c, for each case is determined in the summary and visualization phase by simply taking an average of the 300 bootstrap iterations while computing the standard deviation yields the associated uncertainty.

Each of the thirteen primary modules and libraries developed for this project are written in accordance with the PEP 8 Style Guide for Python Code [16] and other similar coding best practices. These writing guidelines are followed with the aim of facilitating the readability, simple usage, and future development of all code snippets. These programs make use of many functions in the standard Python library, the Maple library of functions, and the PyPI extended library[17] to avoid rewriting already-scrutinized code. In the case where libraries of broad utility are needed but not found to be available in the literature or through easily accessible or free open source collections, they are developed in this work and coauthored with fellow research group member Travis Valdez. Two such modules, sigfig.py and travfit.f, are developed with the intention of world-wide sharing through submission to the PyPI library database with hopeful inclusion in the Python standard library in the case of sigfig.py and hosting on to the research group's website (`http://drake.sharcnet.ca`) for both. Sigfig.py is a library of many functions, one of which rounds a value based on either the given uncertainty of that value or the number of significant figures requested, while Travfit.f is a FORTRAN program which uses quadruple precision arithmetic to perform

least squares fitting for a given polynomial and given set of input data points.

Table 4.1: List of program files ordered according to execution with length, revision number, and brief description.

name	length	rev.	description
Dpoldlz.f	3,767 lines	3	Atomic Energy calculator for given Ω, Z
DP.py	247 lines	4	Input and output management for Dpoldlz.f
DPb.py	82 lines	6	Ω, Z range selector and iteration control for DP.py
dp_inc.py	438 lines	2	Atomic Energy I/O and database management library
Zen.py	37 lines	2	Summary of Energy for each Z and each Ω
EOcon.mw	47 lines	4	Energy extrapolation for each Z
EZDfit.py	233 lines	8	Extrapolation and curve fitting routine with bootstrapping
ez_inc.py	188 lines	6	library of functions used in EZDfit.py
travfit.f	80 lines	2	linear least squares fitting routine
mikez.py	214 lines	5	library of broad useful functions
sigfig.py	448 lines	9	library of functions used in number rounding and display

Chapter 5

Results

In total 161 different nuclear charges were analyzed in the range $Z = .915 \ldots 1.500$. The resulting energies are plotted as a function of nuclear charge and displayed below in figure 5.1 with values in table A.1. The uncertainties are too small to be visible (at most $O(10^{-13})$ au corresponding to $10^{-10}\%$ of the figure height or about 100 pm) yet result in significant variations in Z_c as will be shown later. Different data subsets are defined and also displayed in figure 5.1 along with domain tabulation done in table 5.1. The total number of data sets defined in table 5.1 is 18 which allows for analysis of Z_c as a function of input data range.

Each of the 18 subsets are fit with 3 separate Puiseux expansions (full-integer, $1/2$-integer, and $1/3$-integer powers) with the number of terms in the expansions ranging from 2 to 20. This results in the calculation of 972 ($18 \times 3 \times 18$) unique Z_c values (all 300 more times each for uncertainty determination via the bootstrap method). An illustrative sample of these results are displayed in this section while the exhaustive tabulation can be found in the appendix.

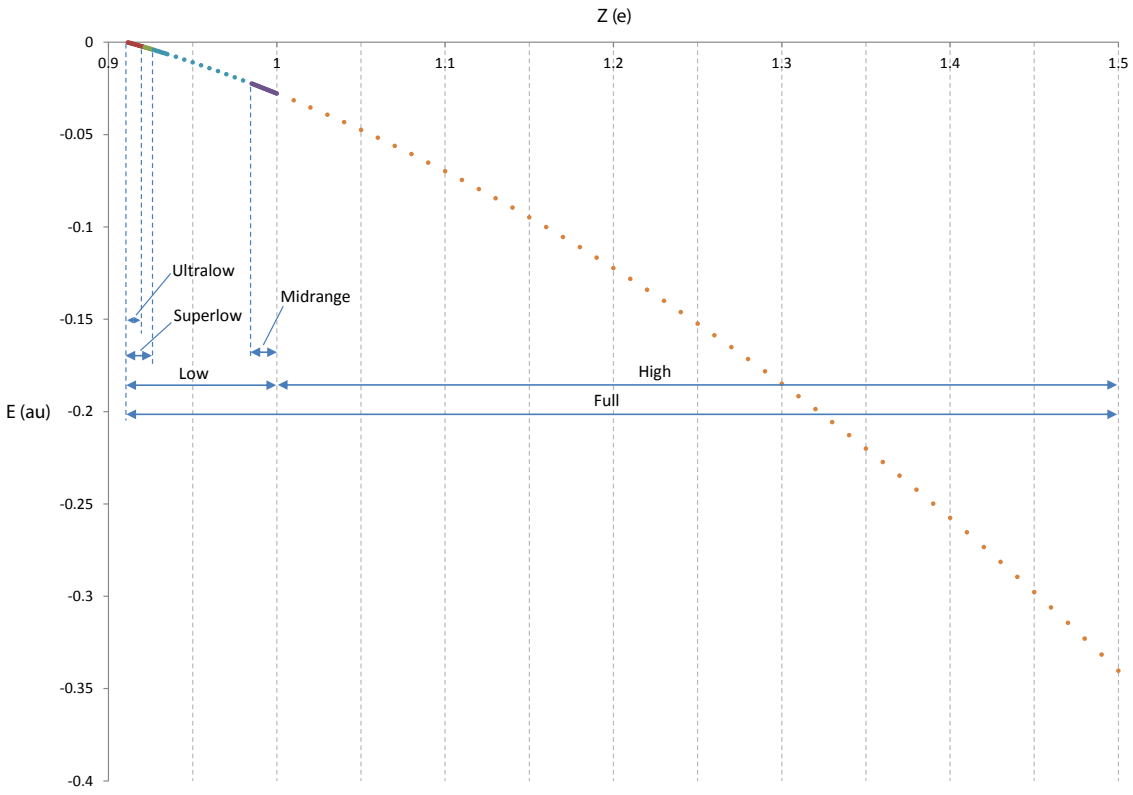

Figure 5.1: Ionization Energy versus Nuclear charge with labelled data subsets.

Table 5.1: Nuclear charge data subsets

Name	Cardinality	Domain	Spacing	further subdivision
Full	161 pts	$Z = 0.911\,5 \ldots 1.500$	variable	even, odd, equidistant (0.01)
High	60 pts	$Z = 1.00 \ldots \quad 1.50$	0.01	even, odd
Low	101 pts	$Z = 0.911\,5 \ldots 1.000$	variable	even, odd, equidistant (0.001)
Midrange	30 pts	$Z = 0.985 \ldots \quad 1.000$	0.0005	even, odd
Superlow	30 pts	$Z = 0.911\,5 \ldots 0.926\,0$	0.000 5	even, odd
Ultralow	20 pts	$Z = 0.911\,5 \ldots 0.921\,0$	0.000 5	

The convergence of Z_c as a function of Puiseux term count is observed in all fits for all data sets. This behaviour is displayed for all fit powers and subdivisions of the Superlow and Ultralow data sets in figure 5.2. Data sets with lower nuclear charge values closer to the Z_c expansion point yield lower and better Z_c estimates. $1/2$-integer power fittings performed the best followed closely by full-integer fittings; $1/3$-integer power fittings were found to perform significantly worse as displayed in figure 5.3. The resulting Z_c is found from the convergence of the $1/2$-power-fit Ultralow and Superlow data sets to be

$$\boxed{Z_c = 0.911\,028\,08(5)} \tag{5.1}$$

as displayed in figure 5.4 and partially tabulated in table 5.2.

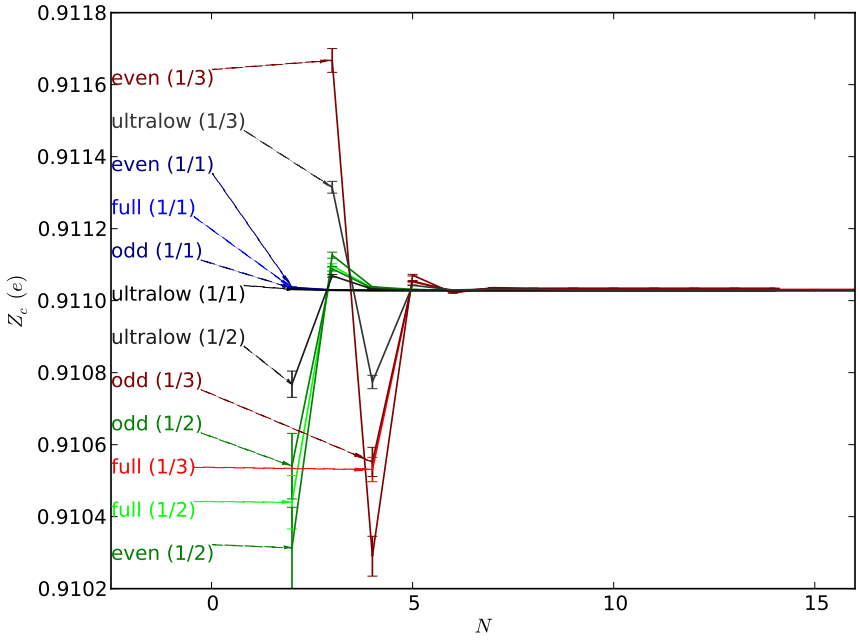

Figure 5.2: Critical Nuclear Charge versus the number of terms included in fitted Puiseux expansion. Each series corresponds to a unique data set chosen from all divisions and fit powers of the Ultralow and Superlow data sets.

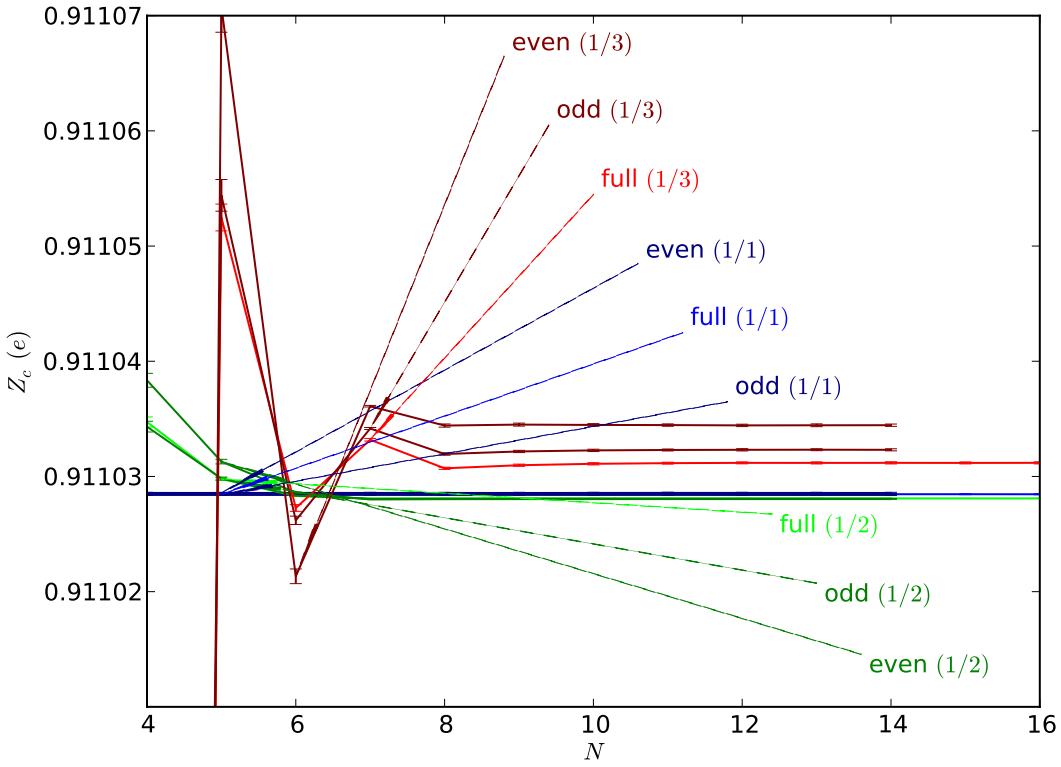

Figure 5.3: Critical Nuclear Charge versus the number of terms included in fitted Puiseux expansion for a narrowed range to resolve the convergence values. Each series corresponds to a unique data set chosen from all divisions and fit power of Ultralow and Superlow data sets.

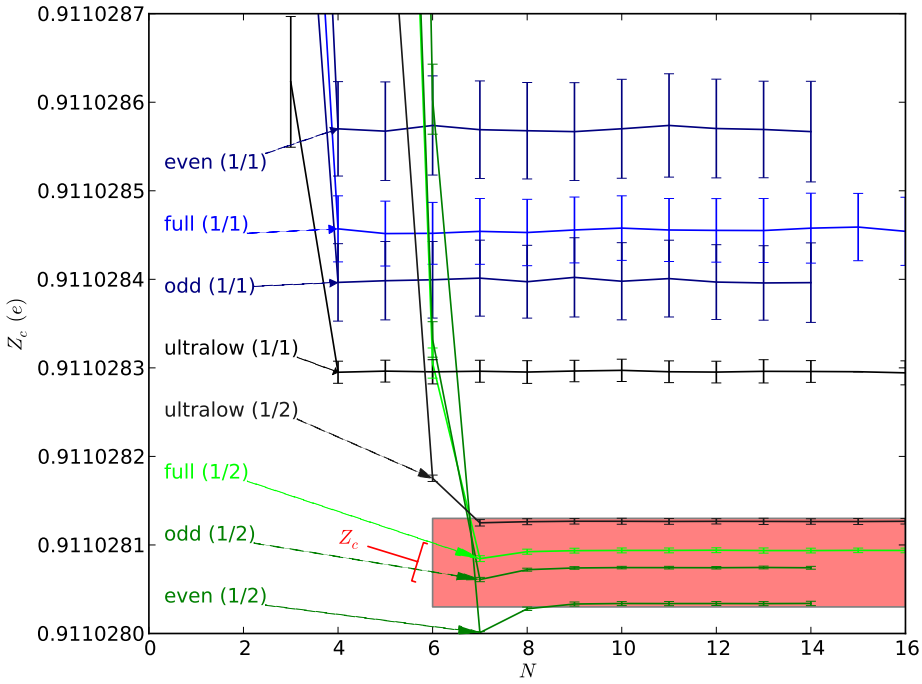

Figure 5.4: Critical Nuclear Charge versus the number of terms included in fitted Puiseux expansion for a narrowed range about Z_c. Ultralow and Superlow data sets are included with limited fit power to $^1/_2$-integer and full-integer fittings.

Table 5.2: Critical Charge Z_c from $^1/_2$-power fit low Z data (summarized)

terms	Ultralow (20)	Superlow (30)	Superlow (odd) (15)	Superlow (even) (15)
6	0.911 028 175 (4)	0.911 028 305 (17)	0.911 028 332 (20)	0.911 028 60 (4)
7	0.911 028 125 (4)	0.911 028 085 (3)	0.911 028 060 9(24)	0.911 028 001 0(11)
8	0.911 028 126 (3)	0.911 028 092 4(29)	0.911 028 072 1(17)	0.911 028 027 9(20)
9	0.911 028 127 (3)	0.911 028 093 6(27)	0.911 028 074 0(15)	0.911 028 033 3(23)
10	0.911 028 127 (3)	0.911 028 093 8(28)	0.911 028 074 4(14)	0.911 028 033 9(24)
11	0.911 028 127 (3)	0.911 028 093 8(27)	0.911 028 074 4(15)	0.911 028 033 8(24)

Chapter 6

Discussion

The largest source of uncertainty in Z_c as seen in figure 5.4 is found to be the choice of input data points used for fitting. Uncertainties from bootstrapping both energy deviations and fit residuals are found to be a few parts in 10^9 while input data choice alters Z_c by at least five parts in 10^8. This prompts a more complete application of the bootstrap which does not yet exist in the literature and consequently lacks proper mathematical justification as will be discussed in the following section.

6.1 Novel bootstrap curve fitting method

In the application of the bootstrap to curve fitting the residuals are resampled with replacement as discussed in section 2.4. This ignores the case where alternate data at different x-values are equally valid and yet would yield deviations in parameters of greater magnitude than simply resampling residuals in accordance with current standard practices. As an illustrative example let us examine a case in this study; $1/2$-integer fitting of the Superlow data set. When all thirty points in this set are included the value of Z_c is seen to converge to 0.911 028 094(3) as illustrated as the third line from the bottom of figure 5.4 (with tabulation done in table 5.2). However, when only the odd values in this set are included Z_c is

seen to converge to 0.911 028 074(1) while even values produce a Z_c of 0.911 028 033(2) (the bottom two lines of figure 5.4). These values differ by parts in 10^8 while their uncertainties from the conventional bootstrap method lie in the range of parts per 10^9. If the selection of data points were arbitrary then these 3 sets spanning the same range with similar or equal density would yield the same result as the standard bootstrap curve fitting method suggests. Clearly this is not the case and it is this that motivates the development and mathematical justification for a novel curve fitting method proposed below.

This new method should draw samples of data points from the existing data set with a weighted preference for data closer to the series expansion point, Z_c. The size of the subsets can be variable but adhering to subsets of half size will give sufficient statistics from which to choose (in this study ${}_{30}C_{15} \approx 155 \times 10^6$ possible subsets). This procedure bears similarity to the delete-d jackknife which is viewed as an approximation to the bootstrap [15] that is shown to lack in scope for the current study. Care will need to be taken to ensure biasses from unrepresentative data sets do not skew results as the mathematical framework is constructed. A fundamental limit to the spacing of data will need to be established where the possible effects of linear dependency can be studied. Internal parameters can also be studied and possibly used for extrapolation. For example, it would be interesting to see if a parameter like Z_c varied as a function of minimum Z or average Z or if perhaps the uncertainty of Z_c exhibited this behaviour and what implications this might have on the method.

6.2 Propagation of Energy Uncertainty

The great precision to which the atomic energy is calculated minimizes the uncertainty of Z_c but at what order of magnitude does the energy uncertainty become a significant factor in the Z_c result? This question can be addressed by artificially manipulating the energy by factors of ten and observing the result. Perturbations of order 10^{-12} au were performed and resulted in altering Z_c by an amount up to 10^{-9}. This represents a significant fraction of the total uncertainty from the bootstrap uncertainty analysis and a fruitful avenue to pursue in order to gain precision in the final result. This factor will likely be less significant in the

proposed jackknife-like analysis where the uncertainty of Z_c will be in the 10^{-8} range but still remains a priority for future work to thoroughly establish a clear relationship between δE and δZ.

Greater accuracy for the energy can be obtained through altering the parameters of

$$\delta E_\infty = \left| \frac{D}{1-(\langle r\rangle + \sigma_r)} - \frac{D}{1-(\langle r\rangle - \sigma_r)} \right|. \tag{2.14}$$

but at the cost of computation time. One low-cost method to yield an increase in precision could be the calculation of Energy for $\Omega < 8$. This could potentially see the deviation in the convergence ratio (σ_r) diminish thus diminishing δE (Eq. 2.14) but this may not be the case. A higher-cost method to unambiguously yield increased precision is the calculation of Energy for $\Omega > 20$. This is guaranteed to produce a decrease in δE by a factor of roughly 3.0 (typical R value) for each increment of maximum Ω since this is, by definition, the projected shrinking of D in Eq. 2.14.

6.3 Wave function behaviour

Analysis of the wave function behaviour as it tends toward the critical charge illustrates the utility of the double basis method. The reciprocals of the nonlinear parameters set the distance scales for the wave function exhibited in Fig. 6.1. The doubled basis set allows for simultaneous representation of both the short-range correlation and the long-range outer electron behaviour. This is a critical feature of the physical model as Z approaches Z_c and the outer electron moves to infinite distance becoming unbound. Other single basis set models require a single set of parameters to describe both the atom's tightly bound hydrogenic behaviour and long range ionization-limit behaviour. This will force the parameters to take compromised values between the two extremes and require a far greater number of terms in the wave function to achieve the same level of accuracy. As term counts inflate so do the linear dependency and stability issues which arise from the diminishing numerical differences between matrix elements. These problems can be alleviated in machines by artificially increasing the size of the floating point memory registers but this is at a high cost to performance since memory register sizes are fixed in hardware and thus require emulation

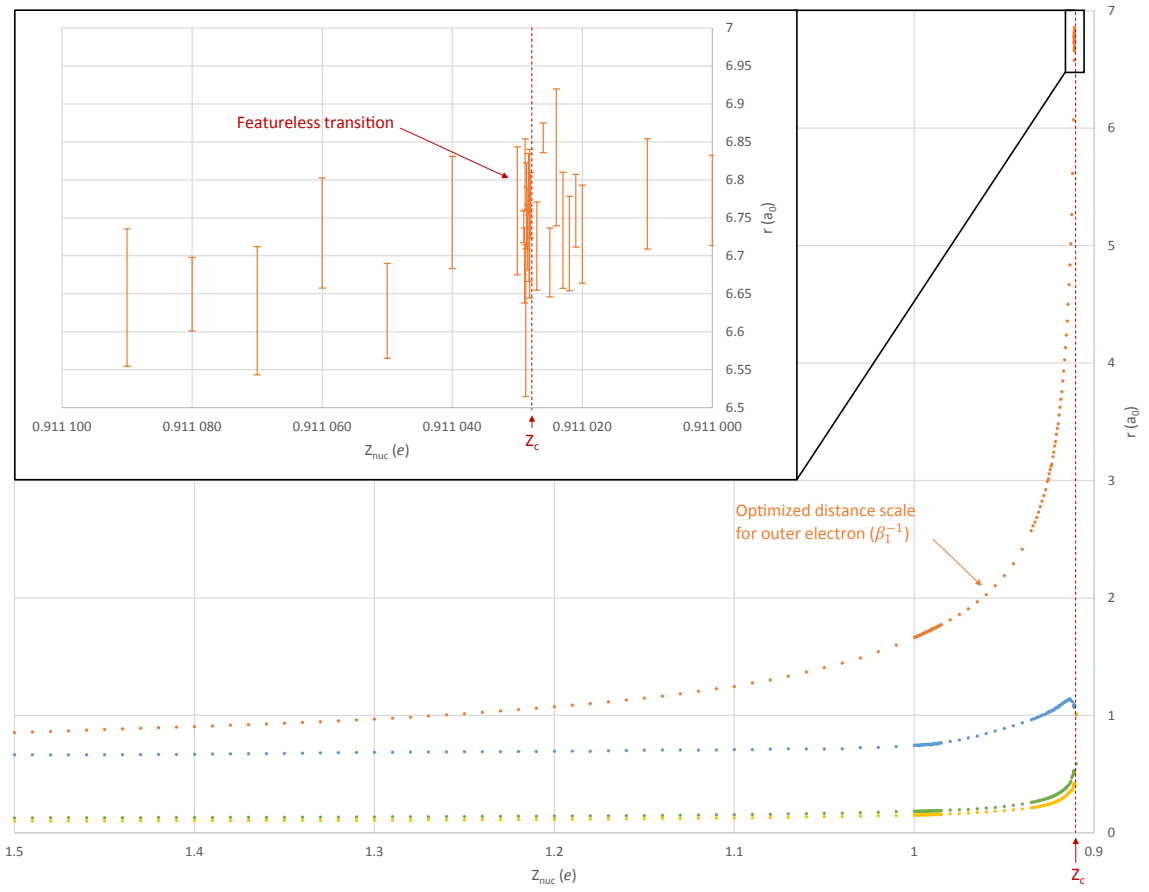

Figure 6.1: Reciprocal nonlinear parameters versus nuclear charge ($\Omega = 20$). $1/\beta_1$ is observed to increase in size as it approaches Z_c but remain finite.

at the software level to increase in capacity. It it not surprising then that other studies have taken far fewer points in the low-Z regime where these effects arising from poor multiple range modelling are prevalent.

6.4 Direct Method of Z_c Determination

An alternative method for obtaining Z_c attempts to avoid extrapolation by simply calculating atomic energies for incrementally lower nuclear charges. The lowest nuclear charge which does not fail to yield a bound state is taken as the critical charge where the uncer-

tainty interval is the difference between the critical charge and highest failed charge. Z_c from this method should be treated as an upper-bound to the actual Z_c since an atomic calculation at $Z \leq Z_c$ will not return a bound state. This was thought to lead to computational problems one might encounter when calculating energies beyond Z_c as work by Turbiner and Guevara indicates [2]. However, preliminary results show an absence of features as the Z_c threshold is crossed using the machine implementation and atomic model in this study. A possible explanation for the lack of threshold effect is the existence of a quasibound state just below Z_c. Further investigation is beyond the scope of this work but is essential for further refinement of the Z_c value.

The direct method employed by Baker et al. [1] is able to yield an upper-bound on Z_c of 0.911 03 beyond which no bound state is found. Using the doubled basis sets of this study and thoughtful analysis of the practical implementation provides a promising avenue for even greater precision in the search for Z_c.

6.5 Comparison with Z_c in literature

The method employed by Guevara and Turbiner [2] extrapolates Z_c from a data set of nine atomic energies by fitting to a $1/2$-power Puiseux expansion (Eq. 2.15) up to power $7/2$ and omitting the $1/2$-power term. The nine atomic energies are calculated using only eight significant digits from the atomic model outlined by Korobov [18] with a machine implementation from Pachucki [19]. Korobov's basis functions are of the form $e^{-\alpha_n^* r_1 - \beta_n^* r_2 - \gamma_n^* r_{12}}$ for a set of quasirandomly generated complex nonlinear parameters and no radial powers. Guevara and Turbiner use nuclear charges $Z \in [1.35, 1.30, 1.25, 1.2, 1.15, 1.10, 1.05, 1.00, 0.95]$ giving a Z_c of 0.910 850 with no stated uncertainty. These results have been reproduced with the machine implementation and atomic model used in this study.

While the method serves as a good preliminary investigation using extrapolation to find Z_c, it lacks atomic energy data close enough to the Z_c expansion point to give a meaningful estimate of the critical charge. Moreover, no clear method for determining a confidence interval for the stated Z_c is presented which leaves much work to be done in assessing its validity. This study expands upon Guevara and Turbiner's work by obtaining the required

low-Z data for meaningful calculation and establishing a method for the determination of uncertainty for Z_c. The increased precision of Z_c to ten significant figures introduces the need for increased precision of atomic energy (discussed in Sect. 6.2) where eight significant figures in energy is shown to be insufficient for ten digits in critical charge. At this level of precision a greater number of fitting terms is shown to also be required for adequate representation as $E(Z)$ is seen to stabilize beyond Puiseux power $^8/_2$ (Fig. 5.4). These high precision methodological advances combined with uncertainty estimation from an extension of the bootstrap address the primary issues from this initiatory investigation.

Values of Z_c in recent literature are presented in Fig. 6.2 where the upper bound determined by Baker [1] (Sect. 6.4) is found to agree with the results of the current work. Older studies not previously mentioned are Stillinger's 1966 investigation estimating $Z_c \cong 0.8941$ [20] and the work by Gustavo et al. estimating $Z_c = 0.9045(35)$ [21]. These works give ratios of disagreement nearly one hundred times greater than that of Drake-Guevara and thousands of times greater than Drake-Baker. The approach uses a method of extrapolation from coefficients of the $1/Z$ expansion which may require a far greater number of terms to yield results of sufficient accuracy.

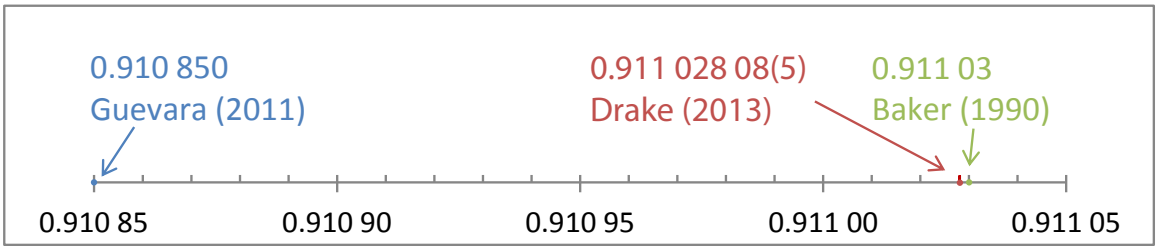

Figure 6.2: Critical Nuclear Charge values in recent literature.

6.6 Future Work

The current study brings to light many promising areas of advancement in the hunt for greater precision of Z_c.

Investigation into a systematic method for the determination of uncertainty is a path

of paramount importance. A method like the extension to the delete-d jackknife discussed in Sect. 6.1 should serve to give a strong interval of confidence for any study involving extrapolation to find Z_c. This proposed method is expected to answer how the critical nuclear charge and its uncertainty change as a function of input atomic energy data.

Further expansion of the energy data set to values closer to Z_c (Sect. 6.4) should prove to be another encouraging avenue of exploration. Careful scrutiny and probable alteration will be required for the methods used to generate these ionization-approaching energy calculations. If this approach is shown to be valid it will likely pave the way for a method of interpolation to determine Z_c. Interpolation is a far superior method of analysis over extrapolation and if possible should act to decrease the uncertainty on Z_c by orders of magnitude.

Advances in statistics and data point selection will necessitate the increase in input atomic energy precision. This precision is achieved by the time-consuming process of collecting energies for a full range of term counts up to perhaps $\Omega = 25$ (Sect. 6.2).

Scrutiny over the $E(Z)$ fitting function is another possible pathway for Z_c advancement. The current machine implementation allows for straightforward evaluation of alternate Puiseux powers with very little effort and small computation time. $1/4$-power fittings are a worthwhile candidate for expansion since the current $1/2$-power terms are a subset of this series. These terms will either provide a better representation of the true charge-energy relationship or add confidence to the current function as the full power and $1/3$-power terms have (Ch. 5). These same principals can be extended to an exponential fit or an attempted fit with initial parameters far from expected values. If the parameters are observed to return to their converged values despite the attempted perturbation then increasing levels of confidence are gained for the method.

Chapter 7

Conclusions

The critical nuclear charge is found with a value of $Z_c = 0.91102808(5)$ where the confidence interval is found to exclude all previous calculations in the literature [2, 1, 21, 20] but with closer agreement to Baker et al. [1]. The increased proximity to Z_c in input data facilitated by the doubled basis set wave functions is shown to yield a sharpened resolution in the final result. The gains in data precision require increased term counts in both the fitting function and wave function to achieve proper convergence as the extrapolation method is pushed to its limits. The bootstrap fitting method is found to be an essential tool for uncertainty analysis and its continued development will give a systematic procedure to further refine the interval of confidence for the critical nuclear charge.

Bibliography

[1] J. D. Baker, D. E. Freund, R. N. Hill, and J. D. Morgan III. *Phys. Rev. A*, 41:1247, 1990.

[2] N. L. Guevara and A. V. Turbiner. Heliumlike and lithiumlike ionic sequences: Critical charges. *Phys. Rev. A*, 84:064501, 2011.

[3] E. A. Hylleraas. *Z. Phys.*, 48:469, 1928.

[4] G. W. F Drake. High-precision calculations for the rydberg states of helium. In F. S. Levin and D. A. Micha, editors, *Long Range Casimir Forces: Theory and Recent Experiments in Atomic Systems*. Plenum Press, 1993.

[5] M. Smith, M. Brodeur, T. Brunner, S. Ettenauer, A Lapierre, R. Ringle, V. L. Ryjkov, F. Ames, P. Bricault, G. W. F. Drake, P. Delheij, D. Lunney, F. Sarazin, and J. Dilling. First penning-trap mass measurement of the exotic halo nucleus ^{11}Li. *Phys. Rev. Lett.*, 101:202501, 2008.

[6] H.A. Bethe and E.E. Salpeeter. *Handbuch der Physik*. Springer-Verlag, Berlin, 1957.

[7] D. J. Griffiths. *Introduction to Quantum Mechanics*. Pearson Education, Inc., second edition, 2005.

[8] E. A. Hylleras and B. Undheim. *ZS. F. Phys.*, 65:759, 1930.

[9] G. W. F. Drake. High precision calculations for helium. In G. W. F. Drake, editor, *Springer Handbook of Atomic, Molecular, and Optical Physics*. Springer Science+Business Media, Inc., 2006.

[10] B. Klahn and W.A. Bingel. *Theor. Chim. Acta*, 44:27, 1977.

[11] B. Klahn and W.A. Bingel. *Int. J. Quantum Chem.*, 11:943, 1978.

[12] E. A. Hylleraas. *Z. Phys.*, 54:347, 1929.

[13] R. A. Nistor. Improved strategies for variational calculations for helium. Master's thesis, University of Windsor, 2004.

[14] H. Margenau and G. Murphy. *The Mathematics of Physics and Chemistry*. D. Van Nostrand Company Inc., 1956.

[15] B. Efron and R.J. Tibshirani. *An Introduction to the Bootstrap*. Chapman & Hall/CRC, 1994.

[16] G. van Rossum, B. Warsaw, and N. Coghlan. Style guide for python code, November 2013. `http://www.python.org/dev/peps/pep-0008/`.

[17] The Python Software Foundation. Python package index, November 2013. `http://pypi.python.org/pypi`.

[18] V. I. Korobov. Coulomb three-body bound-state problem: Variational calculations of nonrelativistic energies. *Phys. Rev. A*, 61:064503, 2000.

[19] K. Pachucki. `http://www.fuw.edu.pl/krp/`, 2011.

[20] F. H. Stillinger Jr. Ground-state energy of two-electron atoms. *J. Chem. Phys.*, 45:3623, 1966.

[21] G. A. Arteca, F. M. Fernndez, and E. A. Castro. Study of eigenvalue singularities from perturbation series: Application to twoelectron atoms. *J. Chem. Phys.*, 84(3):1624–1628, 1986.

Appendix A

Tabulation

Table A.1: Atomic Energy as a function of nuclear charge for the two-electron system.

Z	E_{ground}	$E_{ionization}$
0.910	−0.413 799 211 37(1)	0.000 250 788 63(1)
0.911 00	−0.414 953 580 735 8(1)	0.000 006 919 264 2(1)
0.911 01	−0.414 965 142 110 3(1)	0.000 004 467 939 7(1)
0.911 020	−0.414 976 703 828 7(2)	0.000 002 016 371 3(2)
0.911 021	−0.414 977 860 019 4(1)	0.000 001 771 201 1(1)
0.911 022	−0.414 979 016 213 6(1)	0.000 001 526 028 4(1)
0.911 023	−0.414 980 172 411 2(2)	0.000 001 280 853 3(2)
0.911 024	−0.414 981 328 612 3(1)	0.000 001 035 675 7(1)
0.911 025	−0.414 982 484 816 8(1)	0.000 001 035 675 7(1)
0.911 026	−0.414 983 641 024 7(1)	0.000 001 035 675 7(1)
0.911 027	−0.414 984 797 236 0(1)	0.000 001 035 675 7(1)
0.911 028 0	−0.414 985 953 450 8(1)	0.000 001 035 675 7(1)
0.911 028 1	−0.414 986 069 072 5(1)	0.000 001 035 675 7(1)
0.911 028 2	−0.414 986 184 694 2(2)	0.000 001 035 675 7(2)
0.911 028 3	−0.414 986 300 316 0(1)	0.000 001 035 675 7(1)
0.911 028 4	−0.414 986 415 937 7(2)	0.000 001 035 675 7(2)
0.911 028 5	−0.414 986 531 559 5(2)	0.000 001 035 675 7(2)
0.911 028 6	−0.414 986 647 181 4(1)	0.000 001 035 675 7(1)
0.911 028 7	−0.414 986 762 803 2(1)	0.000 001 035 675 7(1)
0.911 028 8	−0.414 986 878 425 2(1)	0.000 001 035 675 7(1)
0.911 028 9	−0.414 986 994 047 1(1)	−0.000 000 165 729 5(1)
0.911 029	−0.414 987 109 669 1(1)	−0.000 000 190 248 6(1)
0.911 03	−0.414 988 265 890 8(1)	−0.000 000 435 440 8(1)
0.911 04	−0.414 999 828 296 4(1)	−0.000 002 887 496 4(1)
0.911 05	−0.415 011 391 045 4(2)	−0.000 005 339 795 4(2)
0.911 06	−0.415 022 954 137 7(2)	−0.000 007 792 337 7(2)
0.911 07	−0.415 034 517 573 1(2)	−0.000 010 245 123 1(2)

Z	E_{ground}	$E_{ionization}$
0.911 08	−0.415 046 081 351 3(1)	−0.000 012 698 151 3(1)
0.911 09	−0.415 057 645 472 3(2)	−0.000 015 151 422 3(2)
0.911 1	−0.415 069 209 935 9(1)	−0.000 017 604 935 9(1)
0.911 5	−0.415 532 067 595 3(1)	−0.000 115 942 595 3(1)
0.912 0	−0.416 111 395 540 02(6)	−0.000 239 395 540 02(6)
0.912 5	−0.416 691 547 807 37(5)	−0.000 363 422 807 37(5)
0.913 0	−0.417 272 509 616 68(4)	−0.000 488 009 616 68(4)
0.913 5	−0.417 854 267 766 29(2)	−0.000 613 142 766 29(2)
0.914 0	−0.418 436 810 346 72(2)	−0.000 738 810 346 72(2)
0.914 5	−0.419 020 126 527 25(2)	−0.000 865 001 527 25(2)
0.915 0	−0.419 604 206 392 13(2)	−0.000 991 706 392 13(2)
0.915 5	−0.420 189 040 811 77(1)	−0.001 118 915 811 77(1)
0.916 0	−0.420 774 621 339 39(1)	−0.001 246 621 339 39(1)
0.916 5	−0.421 360 940 126 662(7)	−0.001 374 815 126 662(7)
0.917 0	−0.421 947 989 854 050(7)	−0.001 503 489 854 050(7)
0.917 5	−0.422 535 763 672 369(5)	−0.001 632 638 672 369(5)
0.918 0	−0.423 124 255 153 492(4)	−0.001 762 255 153 492(4)
0.918 5	−0.423 713 458 248 168(4)	−0.001 892 333 248 168(4)
0.919 0	−0.424 303 367 249 812(3)	−0.002 022 867 249 812(3)
0.919 5	−0.424 893 976 763 070(3)	−0.002 153 851 763 070(3)
0.920 0	−0.425 485 281 676 422(2)	−0.002 285 281 676 422(2)
0.920 5	−0.426 077 277 138 151(2)	−0.002 417 152 138 151(2)
0.921 0	−0.426 669 958 535 112(2)	−0.002 549 458 535 112(2)
0.921 5	−0.427 263 321 473 944(2)	−0.002 682 196 473 944(2)
0.922 0	−0.427 857 361 764 315(2)	−0.002 815 361 764 315(2)
0.922 5	−0.428 452 075 403 954(2)	−0.002 948 950 403 954(2)
0.923 0	−0.429 047 458 565 205(1)	−0.003 082 958 565 205(1)
0.923 5	−0.429 643 507 582 920(2)	−0.003 217 382 582 920(2)
0.924 0	−0.430 240 218 943 511(1)	−0.003 352 218 943 511(1)
0.924 5	−0.430 837 589 275 022(1)	−0.003 487 464 275 022(1)
0.925 0	−0.431 435 615 338 111(1)	−0.003 623 115 338 111(1)
0.925 5	−0.432 034 294 017 812(1)	−0.003 759 169 017 812(1)
0.926	−0.432 633 622 316 015 1(9)	−0.003 895 622 316 015 1(9)
0.927	−0.433 834 216 318 957 1(8)	−0.004 169 716 318 957 1(8)
0.928	−0.435 037 375 450 742 4(7)	−0.004 445 375 450 742 4(7)
0.929	−0.436 243 079 297 169 5(7)	−0.004 722 579 297 169 5(7)
0.930	−0.437 451 308 772 304 7(5)	−0.005 001 308 772 304 7(5)
0.931	−0.438 662 045 986 297 1(5)	−0.005 281 545 986 297 1(5)
0.932	−0.439 875 274 130 956 3(5)	−0.005 563 274 130 956 3(5)
0.933	−0.441 090 977 380 116 4(4)	−0.005 846 477 380 116 4(4)
0.934	−0.442 309 140 802 391 1(4)	−0.006 131 140 802 391 1(4)
0.935	−0.443 529 750 284 392 8(4)	−0.006 417 250 284 392 8(4)
0.940	−0.449 669 043 929 678 9(3)	−0.007 869 043 929 678 9(3)
0.945	−0.455 867 742 047 676 0(2)	−0.009 355 242 047 676 0(2)
0.950	−0.462 124 699 683 824 4(2)	−0.010 874 699 683 824 4(2)
0.955	−0.468 438 987 351 438 4(2)	−0.012 426 487 351 438 4(2)
0.960	−0.474 809 835 078 199 4(1)	−0.014 009 835 078 199 4(1)
0.965	−0.481 236 594 641 898 2(1)	−0.015 624 094 641 898 2(1)
0.970	−0.487 718 713 047 227 2(1)	−0.017 268 713 047 227 2(1)
0.975	−0.494 255 713 290 746 99(9)	−0.018 943 213 290 746 99(9)

Z	E_{ground}	$E_{ionization}$
0.980	−0.500 847 180 037 978 13(8)	−0.020 647 180 037 978 13(8)
0.985	−0.507 492 748 719 098 95(7)	−0.022 380 248 719 098 95(7)
0.985 5	−0.508 160 268 458 267 51(7)	−0.022 555 143 458 267 51(7)
0.986 0	−0.508 828 325 663 657 18(7)	−0.022 730 325 663 657 18(7)
0.986 5	−0.509 496 920 037 538 18(7)	−0.022 905 795 037 538 18(7)
0.987 0	−0.510 166 051 285 607 39(7)	−0.023 081 551 285 607 39(7)
0.987 5	−0.510 835 719 116 932 63(7)	−0.023 257 594 116 932 63(7)
0.988 0	−0.511 505 923 243 898 22(7)	−0.023 433 923 243 898 22(7)
0.988 5	−0.512 176 663 382 151 75(9)	−0.023 610 538 382 151 75(9)
0.989 0	−0.512 847 939 250 551 71(7)	−0.023 787 439 250 551 71(7)
0.989 5	−0.513 519 750 571 116 84(7)	−0.023 964 625 571 116 84(7)
0.990 0	−0.514 192 097 068 975 76(7)	−0.024 142 097 068 975 76(7)
0.990 5	−0.514 864 978 472 318 24(7)	−0.024 319 853 472 318 24(7)
0.991 0	−0.515 538 394 512 347 26(7)	−0.024 497 894 512 347 26(7)
0.991 5	−0.516 212 344 923 232 08(6)	−0.024 676 219 923 232 08(6)
0.992 0	−0.516 886 829 442 062 32(7)	−0.024 854 829 442 062 32(7)
0.992 5	−0.517 561 847 808 802 90(6)	−0.025 033 722 808 802 90(6)
0.993 0	−0.518 237 399 766 250 07(6)	−0.025 212 899 766 250 07(6)
0.993 5	−0.518 913 485 059 988 06(6)	−0.025 392 360 059 988 06(6)
0.994 0	−0.519 590 103 438 346 86(6)	−0.025 572 103 438 346 86(6)
0.994 5	−0.520 267 254 652 360 75(6)	−0.025 752 129 652 360 75(6)
0.995 0	−0.520 944 938 455 727 60(6)	−0.025 932 438 455 727 60(6)
0.995 5	−0.521 623 154 604 769 09(6)	−0.026 113 029 604 769 09(6)
0.996 0	−0.522 301 902 858 391 61(6)	−0.026 293 902 858 391 61(6)
0.996 5	−0.522 981 182 978 047 86(2)	−0.026 475 057 978 047 86(2)
0.997 0	−0.523 660 994 727 700 06(6)	−0.026 656 494 727 700 06(6)
0.997 5	−0.524 341 337 873 781 65(6)	−0.026 838 212 873 781 65(6)
0.998 0	−0.525 022 212 185 162 70(6)	−0.027 020 212 185 162 70(6)
0.998 5	−0.525 703 617 433 113 75(6)	−0.027 202 492 433 113 75(6)
0.999 0	−0.526 385 553 391 271 25(6)	−0.027 385 053 391 271 25(6)
0.999 5	−0.527 068 019 835 603 52(6)	−0.027 567 894 835 603 52(6)
1.00	−0.527 751 016 544 377 32(6)	−0.027 751 016 544 377 32(6)
1.01	−0.541 521 983 821 166 49(5)	−0.031 471 983 821 166 49(5)
1.02	−0.555 503 408 151 640 55(5)	−0.035 303 408 151 640 55(5)
1.03	−0.569 693 974 922 935 21(4)	−0.039 243 974 922 935 21(4)
1.04	−0.584 092 583 817 748 60(4)	−0.043 292 583 817 748 60(4)
1.05	−0.598 698 303 952 974 89(3)	−0.047 448 303 952 974 89(3)
1.06	−0.613 510 340 534 909 42(3)	−0.051 710 340 534 909 42(3)
1.07	−0.628 528 009 559 125 27(3)	−0.056 078 009 559 125 27(3)
1.08	−0.643 750 718 271 894 44(3)	−0.060 550 718 271 894 44(3)
1.09	−0.659 177 949 847 755 90(3)	−0.065 127 949 847 755 90(3)
1.10	−0.674 809 251 210 729 44(2)	−0.069 809 251 210 729 44(2)
1.11	−0.690 644 223 238 443 26(2)	−0.074 594 223 238 443 26(2)
1.12	−0.706 682 512 799 104 81(2)	−0.079 482 512 799 104 81(2)
1.13	−0.722 923 806 216 715 18(2)	−0.084 473 806 216 715 18(2)
1.14	−0.739 367 823 862 343 38(2)	−0.089 567 823 862 343 38(2)
1.15	−0.756 014 315 642 643 57(2)	−0.094 764 315 642 643 57(2)
1.16	−0.772 863 057 210 182 09(2)	−0.100 063 057 210 182 09(2)
1.17	−0.789 913 846 759 540 62(2)	−0.105 463 846 759 540 62(2)
1.18	−0.807 166 502 302 616 82(2)	−0.110 966 502 302 616 82(2)

Z	E_{ground}	$E_{ionization}$
1.19	−0.824 620 859 338 826 73(1)	−0.116 570 859 338 826 73(1)
1.20	−0.842 276 768 852 953 60(2)	−0.122 276 768 852 953 60(2)
1.21	−0.860 134 095 586 550 08(1)	−0.128 084 095 586 550 08(1)
1.22	−0.878 192 716 539 061 65(1)	−0.133 992 716 539 061 65(1)
1.23	−0.896 452 519 662 907 41(1)	−0.140 002 519 662 907 41(1)
1.24	−0.914 913 402 723 148 42(1)	−0.146 113 402 723 148 42(1)
1.25	−0.933 575 272 297 479 85(1)	−0.152 325 272 297 479 85(1)
1.26	−0.952 438 042 896 388 21(1)	−0.158 638 042 896 388 21(1)
1.27	−0.971 501 636 186 636 79(1)	−0.165 051 636 186 636 79(1)
1.28	−0.990 765 980 303 947 65(1)	−0.171 565 980 303 947 65(1)
1.29	−1.010 231 009 242 963 24(1)	−0.178 181 009 242 963 24(1)
1.30	−1.029 896 662 314 394 23(1)	−0.184 896 662 314 394 23(1)
1.31	−1.049 762 883 660 769 31(1)	−0.191 712 883 660 769 31(1)
1.32	−1.069 829 621 823 457 46(1)	−0.198 629 621 823 457 46(1)
1.33	−1.090 096 829 354 681 08(1)	−0.205 646 829 354 681 08(1)
1.34	−1.110 564 462 469 117 78(1)	−0.212 764 462 469 117 78(1)
1.35	−1.131 232 480 730 429 25(1)	−0.219 982 480 730 429 25(1)
1.36	−1.152 100 846 768 681 704(9)	−0.227 300 846 768 681 704(9)
1.37	−1.173 169 526 025 154 175(9)	−0.234 719 526 025 154 175(9)
1.38	−1.194 438 486 521 483 655(9)	−0.242 238 486 521 483 655(9)
1.39	−1.215 907 698 650 482 868(7)	−0.249 857 698 650 482 868(7)
1.40	−1.237 577 134 986 298 412(9)	−0.257 577 134 986 298 412(9)
1.41	−1.259 446 770 111 862 198(8)	−0.265 396 770 111 862 198(8)
1.42	−1.281 516 580 461 835 231(8)	−0.273 316 580 461 835 231(8)
1.43	−1.303 786 544 179 455 673(8)	−0.281 336 544 179 455 673(8)
1.44	−1.326 256 640 985 887 663(8)	−0.289 456 640 985 887 663(8)
1.45	−1.348 926 852 060 827 978(8)	−0.297 676 852 060 827 978(8)
1.46	−1.371 797 159 933 267 472(7)	−0.305 997 159 933 267 472(7)
1.47	−1.394 867 548 381 426 545(8)	−0.314 417 548 381 426 545(8)
1.48	−1.418 138 002 340 990 938(8)	−0.322 938 002 340 990 938(8)
1.49	−1.441 608 507 820 868 133(8)	−0.331 558 507 820 868 133(8)
1.50	−1.465 279 051 825 767 302(8)	−0.340 279 051 825 767 302(8)

[1]

[1]Note that charge values below $Z = 0.911\,5$ still require thorough analytic scrutiny and may not be converging on the correct root as discussed in section 6.4. As such, energies for $E(Z < 0.9115)$ are presented only as preliminary calculations and are not used in this studies analysis to determine Z_c.

Table A.2: Critical Charge Z_c from 1/2-power fit low Z data (complete).

terms	Ultralow (20)	Superlow (30)	Superlow (odd) (15)	Superlow (even) (15)
2	0.910 77 (4)	0.910 44 (7)	0.910 54 (9)	0.910 31 (11)
3	0.911 069 (4)	0.911 097 (5)	0.911 089 (6)	0.911 126 (9)
4	0.911 032 07 (28)	0.911 034 7(4)	0.911 034 3(5)	0.911 038 3(6)
5	0.911 028 91 (5)	0.911 029 78 (13)	0.911 029 82 (12)	0.911 031 29 (20)
6	0.911 028 175 (4)	0.911 028 305 (17)	0.911 028 332 (20)	0.911 028 60 (4)
7	0.911 028 125 (4)	0.911 028 085 (3)	0.911 028 060 9(24)	0.911 028 001 0(11)
8	0.911 028 126 (3)	0.911 028 092 4(29)	0.911 028 072 1(17)	0.911 028 027 9(20)
9	0.911 028 127 (3)	0.911 028 093 6(27)	0.911 028 074 0(15)	0.911 028 033 3(23)
10	0.911 028 127 (3)	0.911 028 093 8(28)	0.911 028 074 4(14)	0.911 028 033 9(24)
11	0.911 028 127 (3)	0.911 028 093 8(27)	0.911 028 074 4(15)	0.911 028 033 8(24)
12	0.911 028 127 (3)	0.911 028 094 1(27)	0.911 028 074 3(14)	0.911 028 033 8(22)
13	0.911 028 127 (4)	0.911 028 093 7(29)	0.911 028 074 6(15)	0.911 028 033 8(23)
14	0.911 028 126 (3)	0.911 028 093 7(27)	0.911 028 074 2(16)	0.911 028 033 9(25)
15	0.911 028 126 (3)	0.911 028 093 9(26)		
16	0.911 028 127 (3)	0.911 028 093 8(26)		
17	0.911 028 127 (3)	0.911 028 094 0(23)		
18	0.911 028 126 6(29)	0.911 028 094 0(27)		
19	0.911 028 127 (3)	0.911 028 093 8(27)		
20		0.911 028 093 9(28)		

Table A.3: Critical Charge Z_c from 1/2-power fit high Z data.

terms	Midrange (31)	Mid (odd) (15)	Mid (even) (16)	Full (129)	Full Odd (64)	Full Even (65)
3	0.926 39 (5)	0.926 40 (7)	0.926 39 (8)			
4	0.910 163 (4)	0.910 162 (5)	0.910 164 (6)	0.910 42 (6)	0.910 38 (9)	0.910 47 (9)
5	0.911 055 3(8)	0.911 055 2(1)	0.911 055 3(9)	0.911 007 (8)	0.911 002 (13)	0.911 010 (11)
6	0.911 369 9(4)	0.911 370 0(6)	0.911 369 9(6)	0.911 085 9(20)	0.911 094 6(26)	0.911 080 (3)
7	0.911 678 1(16)	0.911 678 7(20)	0.911 678 0(22)	0.911 071 9(21)	0.911 082 (3)	0.911 067 1(25)
8	0.911 876 0(26)	0.911 877 (3)	0.911 876 (3)	0.911 054 7(13)	0.911 062 4(19)	0.911 051 7(18)
9	0.911 978 (3)	0.911 979 (4)	0.911 978 (4)	0.911 041 8(8)	0.911 047 2(11)	0.911 040 4(10)
10	0.912 021 (3)	0.912 022 (4)	0.912 021 (4)	0.911 034 8(4)	0.911 037 9(7)	0.911 034 1(5)
11	0.912 035 (3)	0.912 037 (4)	0.912 036 (4)	0.911 030 95 (20)	0.911 032 7(4)	0.911 030 71 (25)
12	0.912 040 (3)	0.912 041 (4)	0.912 040 (5)	0.911 028 96 (8)	0.911 029 71 (16)	0.911 028 89 (1)
13	0.912 041 (4)	0.912 042 (4)	0.912 041 (4)	0.911 028 114 (29)	0.911 028 34 (7)	0.911 028 10 (4)
14	0.912 041 (3)	0.912 042 (4)	0.912 041 (4)	0.911 027 783 (1)	0.911 027 696 (27)	0.911 027 765 (11)
15	0.912 042 (3)		0.912 041 (5)	0.911 027 886 (14)	0.911 027 93 (4)	0.911 027 865 (18)
16	0.912 041 (3)			0.911 028 017 (23)	0.911 028 19 (6)	0.911 027 988 (29)
17	0.912 041 (3)			0.911 027 791 (8)	0.911 027 666 (18)	0.911 027 773 (8)
18	0.912 041 (3)			0.911 027 839 (9)	0.911 027 787 (29)	0.911 027 820 (1)
19	0.912 041 (3)			0.911 027 899 (12)	0.911 027 92 (4)	0.911 027 876 (14)
20	0.912 041 (3)			0.911 027 788 (8)	0.911 028 07 (5)	0.911 027 937 (20)

Table A.4: Critical Charge Z_c from full-power fit low Z data.

terms	Ultralow (20)	Superlow (30)	Superlow (odd) (15)	Superlow (even) (15)
2	0.911 031 3(5)	0.911 035 6(1 1)	0.911 034 5(1 6)	0.911 036 9(1 6)
3	0.911 028 62(7)	0.911 029 35(17)	0.911 029 12(21)	0.911 029 71(27)
4	0.911 028 295(12)	0.911 028 46(4)	0.911 028 40(4)	0.911 028 57(5)
5	0.911 028 296(12)	0.911 028 45(4)	0.911 028 40(4)	0.911 028 57(6)
6	0.911 028 296(14)	0.911 028 45(4)	0.911 028 40(4)	0.911 028 57(6)
7	0.911 028 296(12)	0.911 028 45(4)	0.911 028 40(4)	0.911 028 57(6)
8	0.911 028 295(13)	0.911 028 45(4)	0.911 028 40(4)	0.911 028 57(5)
9	0.911 028 296(12)	0.911 028 46(4)	0.911 028 40(5)	0.911 028 57(6)
10	0.911 028 297(13)	0.911 028 46(4)	0.911 028 40(4)	0.911 028 57(6)
11	0.911 028 296(12)	0.911 028 46(4)	0.911 028 40(4)	0.911 028 57(6)
12	0.911 028 295(12)	0.911 028 46(4)	0.911 028 40(4)	0.911 028 57(6)
13	0.911 028 296(13)	0.911 028 46(4)	0.911 028 40(4)	0.911 028 57(6)
14	0.911 028 296(12)	0.911 028 46(4)	0.911 028 40(5)	0.911 028 57(6)
15	0.911 028 295 639 0(5)	0.911 028 46(4)		
16	0.911 028 294(14)	0.911 028 45(4)		
17	0.911 028 296(13)	0.911 028 45(4)		
18	0.911 028 296(13)	0.911 028 45(4)		
19	0.911 028 295(12)	0.911 028 45(4)		
20		0.911 028 46(3)		

Table A.5: Critical Charge Z_c from full-power fit high Z data.

terms	Midrange (31)	Mid (odd) (15)	Mid (even) (16)	Full (102)	Full Odd (51)	Full Even (51)
2	0.912 427(6)	0.912 427(8)	0.912 426(8)	0.912 31(12)	0.912 34(17)	0.912 28(18)
3	0.911 755 9(2 5)	0.911 756(3)	0.911 756(4)	0.911 71(6)	0.911 7(1)	0.911 68(9)
4	0.911 448 2(1 3)	0.911 448 5(1 6)	0.911 448 0(1 8)	0.911 40(3)	0.911 42(5)	0.911 39(5)
5	0.911 457 8(1 4)	0.911 458 1(1 8)	0.911 291 3(1 0)	0.911 252(19)	0.911 259(26)	0.911 242(26)
6	0.911 297 0(8)	0.911 459 1(1 7)	0.911 296 9(1 0)	0.911 160(12)	0.911 168(17)	0.911 153(17)
7	0.911 297 7(7)	0.911 459 0(1 9)	0.911 297 8(1 1)	0.911 107(7)	0.911 110(11)	0.911 101(10)
8	0.911 297 7(8)	0.911 458 9(1 9)	0.911 298(1)	0.911 075(5)	0.911 078(6)	0.911 072(6)
9	0.911 297 7(8)	0.911 459 1(1 8)	0.911 297 6(9)	0.911 059(3)	0.911 061(4)	0.911 056(4)
10	0.911 297 7(8)	0.911 459 1(1 9)	0.911 297 6(1 1)	0.911 048 4(2 1)	0.911 050 0(2 9)	0.911 046 4(2 9)
11	0.911 297 7(7)	0.911 458 8(1 8)	0.911 298(1)	0.911 042 2(1 3)	0.911 043 4(1 9)	0.911 040 6(1 9)
12	0.911 297 7(8)	0.911 459 0(1 8)	0.911 297 7(1 0)	0.911 037 9(1 0)	0.911 038 7(1 4)	0.911 036 7(1 3)
13	0.911 297 7(7)	0.911 459 0(1 9)	0.911 297 5(1 0)	0.911 035 1(7)	0.911 036(1)	0.911 034 2(9)
14	0.911 297 7(8)	0.911 458 9(1 8)	0.911 297 8(1 1)	0.911 035 8(8)	0.911 036(1)	0.911 034 6(1 1)
15	0.911 297 7(8)		0.911 297 7(1 0)	0.911 036 2(8)	0.911 037 0(1 1)	0.911 035(1)
16	0.911 297 7(8)			0.911 033 9(6)	0.911 037 4(1 3)	0.911 035 7(1 1)
17	0.911 297 7(7)			0.911 034 3(6)	0.911 034 8(9)	0.911 033 3(9)
18	0.911 297 7(8)			0.911 034 6(7)	0.911 035 1(9)	0.911 033 6(7)
19	0.911 297 7(7)			0.911 034 9(6)	0.911 035 4(9)	0.911 033 9(9)
20	0.911 297 7(8)			0.911 035 1(7)	0.911 035 7(9)	0.911 033 9(9)

Table A.6: Critical Charge Z_c from $1/3$-power fit low Z data.

terms	Ultralow (20)	Superlow (30)	Superlow (odd) (15)	Superlow (even) (15)
2				
3	0.911 315(16)			0.911 67(3)
4	0.910 774(19)	0.910 53(3)	0.910 55(4)	0.910 29(6)
5	0.911 042 8(6)	0.911 052 5(1 2)	0.911 054 4(1 4)	0.911 070 8(2 2)
6	0.911 029 73(9)	0.911 027 26(29)	0.911 026 2(4)	0.911 021 3(6)
7	0.911 031 84(10)	0.911 033 19(11)	0.911 034 16(9)	0.911 036 10(7)
8	0.911 031 66(8)	0.911 030 71(1)	0.911 031 95(11)	0.911 034 42(14)
9	0.911 029 67(6)	0.911 031 0(1)	0.911 032 2(1)	0.911 034 50(13)
10	0.911 029 80(6)	0.911 031 1(1)	0.911 032 26(10)	0.911 034 47(12)
11	0.911 029 85(6)	0.911 031 16(8)	0.911 032 30(9)	0.911 034 46(10)
12	0.911 029 86(6)	0.911 031 18(8)	0.911 032 31(10)	0.911 034 43(10)
13	0.911 029 87(6)	0.911 031 18(9)	0.911 032 32(8)	0.911 034 44(12)
14	0.911 029 86(6)	0.911 031 18(9)	0.911 032 31(9)	0.911 034 45(10)
15	0.911 029 87(6)	0.911 031 17(9)		
16	0.911 029 86(6)	0.911 031 18(9)		
17	0.911 029 87(6)	0.911 031 17(9)		
18	0.911 029 87(6)	0.911 031 18(9)		
19	0.911 029 87(6)	0.911 031 18(9)		
20		0.911 031 18(9)		

Table A.7: Critical Charge Z_c from $1/3$-power fit high Z data.

terms	Midrange (31)	Mid (odd) (15)	Mid (even) (16)	Full (102)	Full Odd (51)	Full Even (51)
2						
3	0.956 62(11)	0.956 65(15)	0.956 60(16)			
4						
5	0.927 71(4)	0.927 73(5)	0.927 71(5)			
6	0.913 105(5)	0.913 106(7)	0.913 105(7)	0.910 869(11)	0.910 880(20)	0.910 864(13)
7	0.898 00(5)	0.897 99(7)	0.898 01(7)	0.910 687(16)	0.910 606(20)	0.910 714(18)
8				0.910 916(7)	0.910 858(12)	0.910 924(9)
9				0.911 016 9(1 4)	0.911 000 9(2 9)	0.911 017 5(1 8)
10				0.911 038 9(3)	0.911 036 0(9)	0.911 039 0(4)
11				0.911 043 88(20)	0.911 047 6(3)	0.911 044 63(20)
12				0.911 042 9(3)	0.911 051 3(4)	0.911 044 5(4)
13				0.911 038 0(4)	0.911 047 1(6)	0.911 039 9(5)
14				0.911 032 28(25)	0.911 048 1(5)	0.911 041 2(4)
15				0.911 034 26(28)	0.911 042 1(5)	0.911 035 9(4)
16				0.911 035 9(3)	0.911 043 9(5)	0.911 037 6(4)
17				0.911 031 29(20)	0.911 045 0(4)	0.911 032 58(28)
18				0.911 032 63(24)	0.911 039 3(5)	0.911 034 1(3)
19				0.911 033 81(23)	0.911 040 8(4)	0.911 035 4(3)
20				0.911 034 82(22)	0.911 042 0(5)	0.911 036 4(3)

VITA AUCTORIS

Born: 1982
B.Sc.: University of Windsor, 2010